

A density functional study of CO adsorption on three- and five-coordinate Al in oxide systems

Konstantin M. Neyman ^{a,1}, Vladimir A. Nasluzov ^{a,2} and Georgii M. Zhidomirov ^b

^a*Lehrstuhl für Theoretische Chemie, Technische Universität München, D-85747 Garching, Germany*

^b*Borisevsk Institute of Catalysis, Russian Academy of Sciences, 630090 Novosibirsk, Russia*

Received 28 March 1996; accepted 14 May 1996

Conventional cluster models of strong and medium strength Lewis acid sites in alumina and zeolites, three-coordinate $[\text{Al}(\text{OH})_3]$ and five-coordinate $[\text{Al}(\text{OH})_3(\text{OH}_2)_2]$ respectively, are studied with the help of a density functional method. A constraint space orbital variation analysis reveals that the charge transfer from probe CO molecules adsorbed on cationic Al centre and the CO polarization comprise essential contributions to the adsorption energy D_e . An analysis of the adsorption-induced C–O frequency shift $\Delta\omega(\text{C–O})$ is also provided. Structural modifications of the Lewis acid sites are considered with respect to their influence on D_e and $\Delta\omega(\text{C–O})$. A comparison of the measured and calculated C–O frequency shifts supports a hypothesis on the existence of Lewis acid sites in oxides in the form of four-coordinate Al cations.

Keywords: coordinatively unsaturated Al ions; Lewis acidity; CO probe; adsorption-induced frequency shifts; cluster models; density functional calculations

1. Introduction

When considering the Lewis acidic strength of aluminas (Al_2O_3) and of zeolites it is common to differentiate between strong and medium power Lewis acid sites (LAS). These two kinds of LAS can be identified using vibrational spectra of adsorption complexes with probe molecules, e.g. with CO [1–4]. Based on the spinel structure of $\gamma\text{-Al}_2\text{O}_3$, the strong LAS are assigned to three-coordinate Al ions, Al_{3c}^{3+} ; precursors are Al ions located at the tetrahedral spinel positions. The LAS of medium strength are ascribed to five-coordinate Al ions, Al_{5c}^{3+} , with the prototype Al species placed in the octahedral spinel sites. This assignment was supported by quantum chemical calculations [5–8]. The theoretical quantification of the relative strength of these LAS was based either on the analysis of their electronic structure [5,7] or on the computed interaction energy with adsorbates [5–7]. Less efforts have been focused so far on rationalizing the difference in the strength of the Al_{3c}^{3+} and Al_{5c}^{3+} LAS with the help of calculated vibrational parameters of the adsorbed probe molecules. In this way a direct comparison to the measured spectroscopic data is possible. For example, a comparative analysis of the experimental and calculated adsorption-induced shifts of the C–N stretching vibrational band of acetonitrile interacting with Al_{3c}^{3+} and Al_{5c}^{3+} centres [8] allowed to delineate dissimilarities between the LAS in HY and ZSM-5 zeolites. Despite the fact that CO molecules belong to the most efficient

probes of the Lewis acidic strength (ref. [1] and references therein), only a few papers deal with first-principles calculations of the C–O frequency shift induced by the adsorption of CO molecules at Lewis centres of coordinatively unsaturated (CUS) aluminium in oxide matrices; among them are communications [4,9] devoted to analysing the vibration of CO on Al_{3c}^{3+} .

The present model cluster density functional (DF) studies of bonding and vibration of CO molecule adsorbed on three- and five-coordinate Al centres (Al_{nc}) in oxides address the following topics: (i) intrinsic uncertainties of the design of cluster models of the Al_{nc}^{3+} LAS ($n = 3, 5$); (ii) the mechanism of CO interaction with Al_{nc}^{3+} LAS in dependence on the coordination number n ; (iii) various contributions to the C–O frequency shift in the Al_{nc}^{3+} –CO adsorption complexes.

A conventional cluster model of the Al_{3c}^{3+} LAS is $\text{Al}(\text{OH})_3$. Of special interest here is the dependence of the adsorption properties of the Al_{3c}^{3+} centre represented by the $\text{Al}(\text{OH})_3$ moiety on the position of the Al cation relative to the plane of the three surrounding oxygen anions, i.e. on the height of the AlO_3 pyramid [10]. A widely used procedure to create Al_{3c}^{3+} centres from tetrahedrally coordinate Al species is to treat the oxide under thermovacuum conditions causing elimination of the hydroxyl groups [11]. One may speculate that the deformation of AlO_3 fragments induced by the removal of an OH group from the tetrahedrally coordinate Al is of negligible importance due to the limited mobility of the oxygen atoms surrounding the Al species in the rigid oxide matrix [9]. Another approach would consist of a full geometry relaxation of the $\text{Al}(\text{OH})_3$ subsystem [8] which is based on the hypothesis of a rather flexible lattice of

¹ E-mail address: neyman@theochem.tu-muenchen.de

² Permanent address: Institute of Chemistry of Natural Organic Materials, Russian Academy of Sciences, 660049 Krasnoyarsk, Russia.

the oxides. Finally, an intermediate procedure corresponds to a change of only the height of the Al atom above the plane of three O atoms, keeping the latter fixed in a position either taken from the experimental bulk structure [6] or determined by results of band structure calculations of the solid [7]. None of the mentioned strategies of the model cluster design seems to have indisputable advantages over the other two approaches. Thus, it is reasonable to evaluate how important the unavoidable variations of the cluster structures are for chemically meaningful features, like adsorption properties. In order to study the dependence of the results calculated for adsorption complexes on the substrate cluster geometry varied within the outlined uncertainty margins, the following three structures of the model cluster $\text{Al}(\text{OH})_3$ are considered: a tetrahedral structure (3a, with the O–Al–O angle of 109.5°), a planar (3c, $\angle(\text{O–Al–O}) = 120^\circ$) and an intermediate one between the former two, 3b, $\angle(\text{O–Al–O}) = 117.1^\circ$, where the Al–O bonds form the angle of 100° with the vertical axis z .

A model $\text{Al}(\text{OH})_3(\text{OH}_2)_2$ of the five-coordinate Al LAS has also been considered in two variants discussed in the literature: one with optimised equal Al–OH and Al–OH₂ distances (5a) [5–7] and another one obtained in the course of an independent variation of the two types of the Al–O bond lengths (5b) [8].

For the models 3b and 5a, which are most adequate from our viewpoint, a constraint space orbital variation (CSOV) analysis has been carried out for the energy of CO adsorption on Al_{3c}^{3+} and Al_{5c}^{3+} centres as well as for the adsorption induced shift of the C–O vibrational frequency.

2. Computational details

The first principles linear combination of Gaussian-type orbitals density functional (LCGTO-DF) cluster method [12] has been used with the parametrization of exchange–correlation interactions suggested by Vosko, Wilk, and Nusair (VWN) [13]. After achieving self-consistency, gradient corrections to the exchange [14] and to the correlation [15,16] energy functionals (BLYP) were computed using the VWN electron density to improve description of the cluster energetics. This “post-hoc” procedure to account for non-local contributions to the exchange–correlation functional has been found [17] to yield essentially the same results as the direct procedure where gradient-corrected potentials are employed self-consistently.

The orbital basis sets and the contraction coefficients for $\text{Al}(12s9p2d) \rightarrow [6s4p2d]$, $\text{C}(9s5p2d) \rightarrow [5s4p2d]$, $\text{O}(9s5p2d) \rightarrow [5s4p2d]$ and $\text{H}(6s2p) \rightarrow [3s2p]$ atoms have been taken from previous LCGTO-DF studies [18–20]. Generalized contractions based on atomic eigenvectors were employed throughout. The two auxiliary basis sets used in the LCGTO-DF method to represent the

electron charge density and the exchange–correlation potential were constructed from the orbital exponents in a standard fashion [12].

A cyclic optimization of the Al–OH and O–H distances as well as of the angle Al–O–H was employed to search for the equilibrium geometry of the cluster $\text{Al}(\text{OH})_3$ (model 3a) under C_{3v} symmetry constraints. The optimised parameters of 1.739 Å, 0.975 Å and 112.8° , respectively, were used in calculations of the other $\text{Al}(\text{OH})_3$ models 3b and 3c (C_{3v} symmetry). For the models of the Al_{5c}^{3+} centres (C_{2v} symmetry group, four oxygen atoms of the AlO_5 fragment are in the plane of the Al atom) only the Al–O distances were varied with the O–H bonds and Al–O–H angles fixed at the values as computed for model 3a; the H_2O parameters $\angle(\text{H–O–H})$ of 103.8° and $r(\text{O–H})$ of 0.979 Å were taken from LCGTO-DF calculations of a free water molecule. This variation resulted in $r(\text{Al–O})$ of 1.862 Å for the distances with both OH and OH₂ ligands (model 5a) or in the $r(\text{Al–O})$ values of 1.795 Å and 2.043 Å, respectively (model 5b). The adsorbed CO molecule was assumed to be oriented upright along the symmetry axis (z axis) of the substrate cluster with the C-atom pointed to the Al cation (fig. 1). Al–CO and C–O distances were optimised in a cyclic fashion with no adsorption-induced change in the substrate cluster geometry taken into account. The Al_{nc}^{3+} –CO binding energy has been corrected for the basis set superposition error (BSSE) with the help of the counterpoise technique [21]. The normal modes of adsorption complexes have been approximated by the computed Al_{nc}^{3+} –CO or C–O internal modes. Anharmonic vibrational frequencies ω (energies of the $0 \rightarrow 1$ transition between the vibrational levels) were computed by fitting a polynomial to seven (C–O mode) or five (Al_{nc}^{3+} –CO mode) points near the minimum of the corresponding potential curve.

The nature of the Al_{nc}^{3+} –CO bonds has been analysed with the help of the CSOV procedure [22] originally proposed in the framework of the HF method and recently employed for the first time in combination with DF studies [18,20,23]. Relevant details of the CSOV procedure are given in section 3.

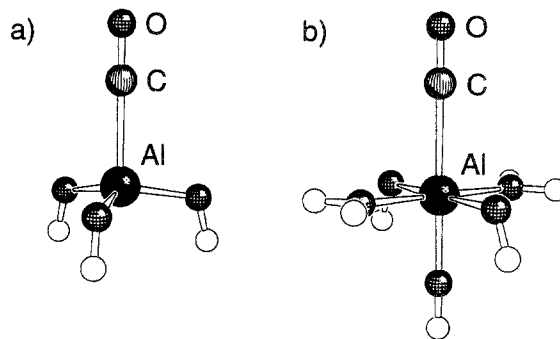


Fig. 1. SCHAKAL [33] representation of the cluster models: (a) $\text{Al}(\text{OH})_3$ (3b)–CO and (b) $\text{Al}(\text{OH})_3(\text{OH}_2)_2$ (5a)–CO.

Table 1

Adsorption energy, structural and vibrational data calculated at the BLYP level for CO adsorbed on LAS Al(OH)₃ and Al(OH)₃(OH₂)₂

Model	$z(\text{Al}-\text{CO})$ (Å)	$\omega(\text{Al}-\text{CO})$ (cm ⁻¹)	$\Delta\omega(\text{C}-\text{O})^a$ (cm ⁻¹)	D_e (eV)	D_e^b (eV)
Al(OH) ₃ (3a)-CO	2.13	236	85	1.09	1.02
Al(OH) ₃ (3b)-CO	2.17	213	84	0.87	0.78
Al(OH) ₃ (3c)-CO	2.27	168	63	0.53	0.45
Al(OH) ₃ (OH ₂) ₂ (5a)-CO	2.28	160	30	0.46	0.34
Al(OH) ₃ (OH ₂) ₂ (5b)-CO	2.24	171	28	0.50	0.37

^a With respect to the value calculated for a free CO molecule, $\omega(\text{C}-\text{O}) = 2120 \text{ cm}^{-1}$.^b After correction for BSSE.

3. Results and discussion

For the cluster models of the Al_{3c}³⁺ centres the constrained geometry optimisation (see section 2) gives the Al–O distance of 1.74 Å which is close to the experimental value of 1.72 Å for tetrahedrally coordinate Al cations in the bulk of aluminum oxide [24]. The Al–O distance optimised for the Al_{5c}³⁺ model 5a with equal Al–O bond lengths, 1.86 Å, is shorter than the value of 1.95 Å measured for Al species in the octahedral position [24]. This deviation is probably due to the firm symmetry constraints imposed on the model 5a.

Results of the calculations of CO adsorption on the series of the considered cluster models of Al_{nc}³⁺ LAS are displayed in table 1. First of all, the close similarity of the results obtained for the models 5a and 5b is evident. Both the adsorption energies of 0.34 and 0.37 eV (1 eV/molecule = 96.48 kJ/mol) and the values of the adsorption-induced frequency shift $\Delta\omega(\text{C}-\text{O})$ of 30 and 28 cm⁻¹, respectively, are almost equal to each other, despite a rather significant structural difference between the cluster models. From these data one may conclude

that inevitable defects of real surfaces accompanied by a modest variation of the Al–O bond lengths and angles do not significantly affect the chemisorption features of the Al_{5c}³⁺ sites relevant for the CO adsorption. A similar conclusion can be drawn for the Al_{3c}³⁺ centres based on the data for the models 3a and 3b. (The planar model 3c is less realistic and thus should not be included in a detailed discussion.) The present DF results definitely support the assignment of the Al_{3c}³⁺ centres to strong LAS and of the Al_{5c}³⁺ sites to LAS of a medium strength: this follows not only from the CO adsorption energies and the frequency shifts $\Delta\omega(\text{C}-\text{O})$, but also from the Al–CO frequencies and bond lengths. Kohn–Sham eigenvalues of the lowest unoccupied levels of the substrate clusters correlate with the strength of their Lewis acidity revealed by the adsorption-related observables. The first empty level of Al(OH)₃ (3b) is at –2.79 eV while it is higher, at –1.64 eV, for the model Al(OH)₃(OH₂)₂ (5a) indicating a reduced electron accepting ability.

The cluster models Al_{3c}³⁺ (3b)-CO and Al_{5c}³⁺ (5a)-CO are likely to be most adequate to represent real surface LAS. Table 2 displays the results of a CSOV analysis of

Table 2

CSOV analysis of various contributions to the interaction energy, ΔE , and to the induced C–O frequency shift with respect to free CO^a, $\Delta^2\omega(\text{C}-\text{O})$, calculated for adsorption complexes of CO with LAS represented by Al(OH)₃ (3b) and by Al(OH)₃(OH₂)₂ (5a) cluster models^b

Interaction channel	Cluster model			
	Al(OH) ₃ (3b)-CO		Al(OH) ₃ (OH ₂) ₂ (5a)-CO	
	ΔE (eV)	$\Delta^2\omega(\text{C}-\text{O})$ (cm ⁻¹)	ΔE (eV)	$\Delta^2\omega(\text{C}-\text{O})$ (cm ⁻¹)
Pauli repulsion + electrostatic	0.13	182	0.33	136
CO polarization	–0.39	–45	–0.19	–25
CO → substrate CT	–0.41	–18	–0.33	–22
substrate polarization	–0.08	0	–0.09	0
substrate → CO CT	–0.12	–36	–0.18	–58
total CSOV	–0.87	83	–0.46	31
SCF	–0.87	84	–0.46	30

^a Calculated for free CO $\omega(\text{C}-\text{O}) = 2120 \text{ cm}^{-1}$.^b No BSSE corrections applied.

the adsorption energy and of the C–O frequency shift for these models.

The CSOV approach attempts to separate and to quantify various contributions to the binding energy of two fragments in a physically meaningful way. The same strategy may also be applied to alterations of other parameters of the supermolecule, like the dipole moment, the vibrational frequencies and the charge transfer, induced by the bond formation between the two parts of a supermolecular system [22]. In the DF CSOV procedure [18,20,23], one starts from the Kohn–Sham orbitals of the separate fragments with their geometries fixed as found in the equilibrium structure of the supermolecule. In CSOV step 1 these orbitals are orthogonalised with respect to each other for the desired interfragment separation. The superimposed fragmental charge densities built of the mentioned orbitals are then used in a supermolecule calculation. The energy difference relative to the sum of the total energies of the isolated fragments is taken to represent the sum of the Pauli repulsion and of the “frozen orbital” electrostatic attraction between the two fragments. In step 2 of the CSOV analysis, the polarization of the adsorbate is investigated by allowing only an orbital variation within the space of the occupied and vacant orbitals of the adsorbate in the presence of the “frozen” substrate. The contribution of the adsorbate-to-substrate charge transfer is then characterized by including the unoccupied substrate orbitals in the variation space (CSOV step 3). The resulting adsorbate orbitals of step 3 are kept frozen during the subsequent steps 4 and 5. The latter steps aim at the evaluation of contributions due to the substrate polarization and to the substrate-to-adsorbate charge transfer, respectively. They are performed in a way analogous to steps 2 and 3. In steps 3 and 5, the charge transfer contributions of orbitals belonging to different irreducible representations may be separated.

It can be seen from table 2 that the σ charge transfer $\text{CO} \rightarrow \text{Al}_{\text{nc}}^{3+}$ contributes substantially to stabilize CO on LAS both of the $\text{Al}_{3\text{c}}^{3+}$ and $\text{Al}_{5\text{c}}^{3+}$ types. The same is valid for the contribution of CO polarization which, however, is somewhat less important for the complex of $\text{Al}_{5\text{c}}^{3+}$. A non-negligible charge transfer in the opposite direction, $\text{Al}_{\text{nc}}^{3+} \rightarrow \text{CO}$, taking place in the π channel, is due to the oxygen ions surrounding the cation under consideration. This interaction component is more significant for the $\text{Al}_{5\text{c}}^{3+}$ moieties having four oxygen neighbours available for interactions with the adsorbate molecule comparing to the three anions attached to $\text{Al}_{3\text{c}}^{3+}$. A similar-bonding mechanism has previously been found in density functional calculations of CO adsorption on top of Mg^{2+} cations at the $\text{MgO}(001)$ surface, carried out within local density [25,26] and gradient corrected [26] approaches.

In agreement with the results reported for adsorption

complexes formed with Brønsted acid centres in zeolites [18] and with ionic metal oxides [20,27], the adsorption-induced increase of the C–O frequency on LAS is caused by the Pauli repulsion contributing 182 and 136 cm^{-1} to the overall calculated blue shift in $\text{Al}_{3\text{c}}^{3+}\text{-CO}$ and $\text{Al}_{5\text{c}}^{3+}\text{-CO}$, respectively. The remaining CSOV components act to reduce the frequency rather similarly for both types of LAS, by 99 cm^{-1} ($\text{Al}_{3\text{c}}^{3+}\text{-CO}$) and 105 cm^{-1} ($\text{Al}_{5\text{c}}^{3+}\text{-CO}$). This means that the basic difference between the resulting C–O frequency shifts in $\text{Al}_{\text{nc}}^{3+}\text{-CO}$ complexes is already present in the first CSOV step, which represents the sum of Pauli repulsion and electrostatic attraction. The stronger electrostatic attraction of CO to $\text{Al}_{3\text{c}}^{3+}$ than to $\text{Al}_{5\text{c}}^{3+}$ species is accompanied by a stronger Pauli repulsion in the former case. This effect is revealed by the more significant increase of the intramolecular frequency of the adsorbed CO. The aforementioned considerations are by no means in contradiction with the finding that the overall energetic balance computed at the first CSOV step is in favour of interactions with $\text{Al}_{3\text{c}}^{3+}$ rather than with $\text{Al}_{5\text{c}}^{3+}$. A large decrease of the shift $\Delta\omega(\text{C-O})$ results from the π charge transfer $\text{Al}_{\text{nc}}^{3+} \rightarrow \text{CO}$ as is to be expected from the weakening of the C–O bond caused by a population of the strongly antibonding $\text{CO } 2\pi^*$ level. Based on similar arguments, the σ charge transfer $\text{CO} \rightarrow \text{Al}_{\text{nc}}^{3+}$ leading to a depopulation of the slightly antibonding $\text{CO } 5\sigma$ orbital might be expected to increase the force constant of the adsorbed CO. However, another consequence of the σ charge transfer is more important because a reduction of the C–O force constant (and of the frequency) is computed for this CSOV step: the σ charge transfer $\text{CO} \rightarrow \text{Al}_{\text{nc}}^{3+}$ causes not only a depopulation of the $\text{CO } 5\sigma$ orbital (resulting in a blue frequency shift in free CO), but also a significant relaxation of the Pauli repulsion responsible for the increased C–O frequency and thus a larger red shift. Therefore, an overall negative value of the C–O frequency shift is associated with the σ channel $\text{CO} \rightarrow \text{Al}_{\text{nc}}^{3+}$.

It would be interesting now to compare the calculated adsorption-induced frequency shifts $\Delta\omega(\text{C-O})$ and the adsorption energies with the experimental data, but the problem of assignment of the observed vibrational bands to a particular type of the surface sites makes this comparison ambiguous. In the vibrational spectra of CO adsorbed on LAS of different types of aluminas the following three regions of bands are usually observed: $2210\text{--}2235\text{ cm}^{-1}$ (A), $2190\text{--}2210\text{ cm}^{-1}$ (B) and $2160\text{--}2190\text{ cm}^{-1}$ (C). The estimated adsorption energies of CO amounts to $0.50\text{--}0.60$, $0.35\text{--}0.45$ and about 0.20 eV [2,3], respectively. Arguments have been presented for ascribing region A to adsorption complexes of CO with the $\text{Al}_{3\text{c}}^{3+}$ centres [28]. However, another assignment of this spectral region, as being due to complexes on defects, became widely accepted later on [2]. Region B has been attributed to adsorption complexes with $\text{Al}_{3\text{c}}^{3+}$ and C region to $\text{Al}_{5\text{c}}^{3+}$ [2]; a similar interpretation was also pro-

posed in ref. [29]. The relative difference between the C–O frequency shifts on various adsorption sites is generally more reliable for a comparison of the computed observables with the experimental data than the absolute frequency values. The calculated difference of about 55 cm^{-1} is rather close to the frequency alteration between the intervals A and C. Based on these results it is reasonable to suggest that region A corresponds to the Al_{3c}^{3+} species and region C manifests the Al_{5c}^{3+} centres. Then, the hypothesis may be put forward proposed that region B is a manifestation of Al_{4c}^{3+} centres, the possible importance of which was already discussed [11,30,31]. However, the present assignment of the vibrational bands which is based on tiny frequency variations (an error of only $10\text{--}20\text{ cm}^{-1}$ would shift the frequency calculated for the complexes of Al_{3c}^{3+} into the region B) still requires further experimental and theoretical validation despite the known good accuracy of the DF cluster methods to reproduce vibrational frequencies [32].

4. Conclusion

The basic results of the present LCGTO-DF model cluster studies of three- and five-coordinate Al^{3+} LAS in oxides and of their adsorption complexes with probe CO molecules can be summarized as follows:

(1) Uncertainties inherent to the cluster model design of the Al_{nc}^{3+} LAS are shown to result in only subordinate alterations of the calculated observables under consideration. A crucial finding is that both CO adsorption energies and the adsorption-induced C–O frequency shifts computed for the two different types of LAS, Al_{3c}^{3+} and Al_{5c}^{3+} , are well separated irrespective of substrate cluster deformations that lie within reasonable limits.

(2) A CSOV analysis of the Al_{nc}^{3+} –CO bonding reveals, besides the electrostatic contribution, a notable energy gain due to the $\text{CO} \rightarrow \text{Al}_{nc}^{3+} \sigma$ charge transfer, which is expected for LAS, as well as a stabilizing contribution of the CO polarization. Both effects are larger for stronger Al_{3c}^{3+} LAS than for Al_{5c}^{3+} ones. A π back donation $\text{Al}_{nc}^{3+} \rightarrow \text{CO}$ which is less common for substrate centres without d orbitals also stabilizes the bond; this is due to the interaction of CO with oxygen anions surrounding Al cations.

(3) The adsorption-induced blue shift of the C–O vibrational frequency is a consequence of the Pauli repulsion between CO and the Al_{nc}^{3+} centre in its oxide surrounding. All other contributions, including a depopulation of the antibonding 5σ orbital of CO, act to decrease the C–O frequency.

(4) A hypothesis on the manifestation of the complexes of CO on the Al_{4c}^{3+} LAS in the spectral region of $2190\text{--}2210\text{ cm}^{-1}$ has been proposed based on a comparison of the calculated vibrational frequencies with experiment. Further studies are required to examine this suggestion.

Acknowledgement

The authors are indebted to Professor N. Rösch for his interest in the project as well as for the possibility to use the computational facilities of his group at TU Munich. This study has been made possible by grants from INTAS and from Volkswagen Foundation (project I/68 691). The work of KN was supported by the Deutsche Forschungsgemeinschaft and by the Bayerische Forschungsverbund Katalyse (FORKAT).

References

- [1] H. Knözinger, in: *Adsorption on Ordered Surfaces of Ionic Solids and Thin Films*, Springer Series in Surface Sciences, Vol. 33, eds. H.-J. Freund and E. Umbach (Springer, Berlin, 1993) p. 257.
- [2] A. Zecchina, E.E. Platero and C.O. Areán, *J. Catal.* 107 (1987) 244.
- [3] E.A. Paukshitis, R.I. Soltanov and E.N. Yurchenko, *React. Kinet. Catal. Lett.* 16 (1981) 93.
- [4] L.M. Kustov, V.B. Kazansky, S. Beran, L. Kubelková and P. Jiru, *J. Phys. Chem.* 91 (1987) 5247.
- [5] M.B. Fleisher, L.O. Golender and M.V. Shimanskaya, *J. Chem. Soc. Faraday Trans.* 87 (1991) 745.
- [6] M. Lindblad and T.A. Pakkanen, *Surf. Sci.* 286 (1993) 333.
- [7] H. Tochikawa and T. Tsuchida, *J. Mol. Catal. A* 96 (1995) 277.
- [8] A.G. Pelmenchikov, R.A. van Santen, J. Jänchen and E. Meijer, *J. Phys. Chem.* 97 (1993) 11071.
- [9] S. Bates and J. Dwyer, *J. Phys. Chem.* 97 (1993) 5897.
- [10] A.G. Pelmenchikov, I.N. Senchenya, G.M. Zhidomirov and V.B. Kazansky, *Kinet. Catal.* 24 (1983) 230.
- [11] E.A. Paukshitis, *Infrared Spectroscopy in Heterogeneous Acid-Base Catalysis* (Nauka, Novosibirsk, 1992) p. 256 (in Russian).
- [12] B.I. Dunlap and N. Rösch, *Adv. Quantum Chem.* 21 (1990) 317.
- [13] S.H. Vosko, L. Wilk and M. Nusair, *Can. J. Phys.* 58 (1980) 1200.
- [14] A.D. Becke, *Phys. Rev. A* 38 (1988) 3098.
- [15] C. Lee, W. Yang and R.G. Parr, *Phys. Rev. B* 37 (1988) 785.
- [16] B. Miehlisch, A. Savin, H. Stoll and H. Preuss, *Chem. Phys. Lett.* 157 (1989) 200.
- [17] L. Fan and T. Ziegler, *J. Chem. Phys.* 94 (1991) 6057.
- [18] K.M. Neyman, P. Strodel, S.P. Ruzankin, N. Schlensog, H. Knözinger and N. Rösch, *Catal. Lett.* 31 (1995) 273.
- [19] P. Strodel, K.M. Neyman, H. Knözinger and N. Rösch, *Chem. Phys. Lett.* 240 (1995) 547.
- [20] K.M. Neyman, S.P. Ruzankin and N. Rösch, *Chem. Phys. Lett.* 246 (1995) 546.
- [21] S.F. Boys and F. Bernardi, *Mol. Phys.* 19 (1970) 553.
- [22] P.S. Bagus, K. Hermann and C.W. Bauschlicher, *J. Chem. Phys.* 80 (1984) 4378.
- [23] K. Albert, K.M. Neyman, V.A. Nasluzov, S.P. Ruzankin, C. Yertzian and N. Rösch, *Chem. Phys. Lett.* 245 (1995) 671.
- [24] R.W.G. Wyckoff, *Crystal Structures*, 2nd Ed., Vol. 4 (Interscience, New York, 1968).
- [25] K.M. Neyman and N. Rösch, *Chem. Phys.* 168 (1992) 267.
- [26] K.M. Neyman and N. Rösch, *Ber. Bunsenges. Phys. Chem.* 96 (1992) 1711.
- [27] G. Pacchioni, G. Cogliandro and P.S. Bagus, *Int. J. Quantum Chem.* 42 (1992) 1115.
- [28] H. Knözinger and P. Ratnasamy, *Catal. Rev. Sci. Eng.* 17 (1978) 31.
- [29] C. Morterra, S. Coluccia, E. Garrone and G. Ghiotti, *J. Chem. Soc. Faraday Trans. I* 75 (1979) 289.
- [30] V. Gruver and J.J. Fripiat, *J. Phys. Chem.* 98 (1994) 8549.

- [31] D. Coster, A.L. Blumenfeld and J.J. Fripiat, J. Phys. Chem. 98 (1994) 6201.
- [32] N. Rösch, in: *Cluster Models for Surface and Bulk Phenomena*, NATO ASI Series B, eds. G. Pacchioni, P.S. Bagus and F. Parmigiani (Plenum Press, New York, 1992) p. 251.
- [33] E. Keller, Program SCHAKAL 92, Kristallographisches Institut der Universität Freiburg, Germany (1992).